







Article

Response Surface Methodology and Artificial Neural Networks-Based Yield Optimization of Biodiesel Sourced from Mixture of Palm and Cotton Seed Oil

Luqman Razzaq¹, Muhammad Mujtaba Abbas^{2,*}, Sajjad Miran¹, Salman Asghar³, Saad Nawaz^{2,*}, Manzoore Elahi M. Soudagar^{4,5}, Nabeel Shaukat⁶, Ibhama Veza⁷, Shahid Khalil⁸, Anas Abdelrahman⁹ and Muhammad A. Kalam¹⁰

- ¹ Department of Mechanical Engineering, University of Gujrat, Gujrat 50700, Pakistan; luqmanrazzaq456@gmail.com (L.R.); sajjad.miran@uog.edu.pk (S.M.)
 - ² Department of Mechanical, Mechatronics and Manufacturing Engineering (New Campus), University of Engineering and Technology (UET), Lahore 54000, Pakistan
 - ³ Department of Product and Industrial Design (PID), University of Engineering and Technology (UET), Lahore 54890, Pakistan; salman.asghar@uet.edu.pk
 - ⁴ Department of Mechanical Engineering, School of Technology, Glocal University, Delhi-Yamunotri Marg, SH-57, Mirzapur Pole 247121, Uttar Pradesh, India; me.soudagar@gmail.com
 - ⁵ Department of Mechanical Engineering, University Centre for Research & Development, Chandigarh University, Mohali 140413, Punjab, India
 - ⁶ Graduate School of Advance Sciences and Engineering, Hiroshima University, Hiroshima 739-8511, Japan; mujtabaueetian@gmail.com
 - ⁷ Faculty of Mechanical Engineering, Universiti Teknikal Malaysia Melaka, Hang Tuah Jaya, Durian Tunggal, Melaka 76100, Malaysia; ibhamveza@utem.edu.my
 - ⁸ Mechanical Engineering Technology, National Skills University, Islamabad 44000, Pakistan; shahid.khalil@nsu.edu.pk
 - ⁹ Department of Mechanical Engineering, Faculty of Engineering & Technology, Future University in Egypt, New Cairo 11845, Egypt; anas.mohamed@fue.edu.eg
 - ¹⁰ Faculty of Engineering and IT, University of Technology, Sydney 2007, Australia; mdabul.kalam@uts.edu.au
- * Correspondence: m.mujtaba@uet.edu.pk (M.M.A.); dr.saadnawaz@uet.edu.pk (S.N.)



Citation: Razzaq, L.; Abbas, M.M.; Miran, S.; Asghar, S.; Nawaz, S.; Soudagar, M.E.M.; Shaukat, N.; Veza, I.; Khalil, S.; Abdelrahman, A.; et al. Response Surface Methodology and Artificial Neural Networks-Based Yield Optimization of Biodiesel Sourced from Mixture of Palm and Cotton Seed Oil. *Sustainability* **2022**, *14*, 6130. <https://doi.org/10.3390/su14106130>

Academic Editor: Elio Dinuccio

Received: 6 April 2022

Accepted: 11 May 2022

Published: 18 May 2022

Publisher's Note: MDPI stays neutral with regard to jurisdictional claims in published maps and institutional affiliations.



Copyright: © 2022 by the authors. Licensee MDPI, Basel, Switzerland. This article is an open access article distributed under the terms and conditions of the Creative Commons Attribution (CC BY) license (<https://creativecommons.org/licenses/by/4.0/>).

Abstract: In this present study, cold flow properties of biodiesel produced from palm oil were improved by adding cotton seed oil into palm oil. Three different mixtures of palm and cotton oil were prepared as P50C50, P60C40, and P70C30. Among three oil mixtures, P60C40 was selected for biodiesel production via ultrasound assisted transesterification process. Physiochemical characteristics—including density, viscosity, calorific value, acid value, and oxidation stability—were measured and the free fatty acid composition was determined via GCMS. Response surface methodology (RSM) and artificial neural network (ANN) techniques were utilized for the sake of relation development among operating parameters (reaction time, methanol-to-oil ratio, and catalyst concentration) ultimately optimizing yield of palm–cotton oil sourced biodiesel. Maximum yield of P60C40 biodiesel estimated via RSM and ANN was 96.41% and 96.67% respectively, under operating parameters of reaction time (35 min), M:O molar ratio (47.5 v/v %), and catalyst concentration (1 wt %), but the actual biodiesel yield obtained experimentally was observed 96.32%. The quality of the RSM model was examined by analysis of variance (ANOVA). ANN model statistics exhibit contented values of mean square error (MSE) of 0.0001, mean absolute error (MAE) of 2.1374, and mean absolute deviation (MAD) of 2.5088. RSM and ANN models provided a coefficient of determination (R^2) of 0.9560 and a correlation coefficient (R) of 0.9777 respectively.

Keywords: biodiesel; palm oil; cotton seed oil; response surface methodology; artificial neural network

1. Introduction

The global demand for petroleum will increase up to 40% by 2025 [1]. Total final energy consumption (TFEC) increased by 25.3 exajoules (EJ), or around 1.4% annually during the 2013–2018 period. In 2017–2018, the transport sector accounted for 32% of the global TFEC and 96.7% of these energy needs were met by using fossil fuels. In 2019, the transport sector accounted for almost one-quarter of the global energy-related greenhouse gas emissions [2]. These growing concerns related to energy demand and environmental problems have urged the researchers and governments to search for alternative fuel sources to conventional ones [3–5]. Biomass sourced liquid biofuels can be the best near-term alternative of fossil fuels and they are also posing a resurgence to oil prices elevation [6]. In recent years, biodiesel use has been increasing because of its advantages such as cheapness, renewability, cleanliness, and reduced level of pollution. Its utilization is safe for the environment as well as vehicular engines due to its similar physicochemical properties to petroleum diesel [7–9]. Global biodiesel market will flourish at a compound annual growth rate (CAGR) of 4.57% during 2017–2021 [10]. However, the market growth is strongly resisted by its production cost. To overcome this, manufacturers and researchers are trying to adopt strategies such as the use of an efficient catalyst, inexpensive and readily available feedstocks, and advanced technologies [11–13].

The global biodiesel production increased 13% in 2019 [14]. Indonesia became the largest producer of biodiesel (17% of global production) followed by the United States (14%), Brazil (12%), Germany (8%), France (6.3%), and Argentina (5.3%) [2]. Soybean and corn are key feedstocks for biodiesel production in The United States, while rapeseed is used in Europe, and palm oil is the prominent feedstock in Asia [15]. Palm has an oil content of 35–55% and a high percentage of saturated fatty acids which makes it a good feedstock for producing biodiesel of better oxidative stability [16]. One serious concern is the low percentage of unsaturated fatty acids which imparts poor cold flow properties to palm oil-based biodiesel [17]. Researchers are enhancing properties via blending of biofuels and addition of synthetic antioxidants [16]. Cottonseed oil has a high unsaturated fatty acids (linoleic acids) percentage which can improve cold flow properties [18]. Thus, it can be blended with palm oil before transesterification for property enhancement [16].

Cost effectiveness and energy-efficiency of ultrasound-assisted transesterification makes it better for biodiesel production [19]. Ultrasound-assisted transesterification consumes less amount of energy than the conventional transesterification [20]. In biodiesel production, ultrasound assisted transesterification is more effective than traditional methods of mixing comparatively. The ultrasound energy enhances the chemical reaction rate of transesterification and ester yield, and it reduces reaction time along with energy consumption [21]. In one study, it was reported that biodiesel yield relies on ultrasonic energy nature and different yield percentages can be obtained with pulse and continuous sonication [20]. Utilizing waste cooking oil, 98% biodiesel yield was obtained via pulse sonication and 93% via continuous sonication [22]. Ultrasound-assisted commercial scale production of biodiesel can be energy and time efficient as well as economical in terms of cost and catalyst usage [16].

Transesterification reaction depends on methanol-to-oil ratio, catalyst concentration, time, and temperature [23]. These parameters directly affect the transesterification process and biodiesel yield [24]. Input parameters' impacts on yield have been extensively analyzed via RSM [3]. This software can be employed to achieve optimum results by obtaining experiment matrix depending on input parameters [25]. A number of researchers have employed RSM for yield optimization via obtaining proper reaction parameters comparison, ultimately saving costs, materials, and time [26]. Dwivedi and Sharma [27] produced biodiesel from Pongamia oil and optimized yield via RSM based Box–Behnken design technique. In another study, process parameters were optimized and consequently 93.81% yield was obtained from WCO sourced biodiesel via Box–Behnken design [28]. To reduce probability of failure and avoid extreme reaction parameter values, Box–Behnken design is

restricted to three levels. Box–Behnken is preferred over central composite-based design due to its cost effectiveness and greater efficiency [29–31].

ANN is an artificial intelligence-based methodology which has acquired massive importance in optimizing esterification and transesterification processes involved in biodiesel production [32–34]. For instance, Betiku and Ajala [35] compared performance of RSM and ANN to produce biodiesel via transesterification of yellow oleander oil. The study demonstrated that ANN provides better optimization rather than RSM in terms of predictive ability and data fitting. In another study, Betiku and Omilakin [36] optimized the process parameters for transesterification of neem oil via RSM and ANN and exhibited that ANN is more efficient. ANN can also be used in combination with other modeling tools for the optimization of process parameters [37]. For instance, Rajendra [38] used ANN along genetic algorithm (GA) to optimize process variables in pretreatment of plant oils to reduce the FFA content. In a recent study, H. Ong and J. Milano used ANN coupled along ant colony optimization (ACO) for yield enhancement [39].

Pakistan lies among the top cotton producing countries with an overall fourth position worldwide [40]. The cotton production was 7.7 and 8.2 million 217.424 kg bales in 2016–2017 and 2017–2018 respectively. Besides using cotton for fiber demands, Pakistan also fulfills its edible oil requirements (18.8%) from cotton seed oil [40]. Being a developing country, Pakistan can utilize this cotton seed oil to produce renewable biofuels such as biodiesel. One major concern which limits using cotton seed oil is the poor oxidative stability of the resulting biodiesel [41]. Palm oil biodiesel cold flow is not too good, but palm biodiesel shows excellent oxidation stability. Therefore, there is a research gap of producing biodiesel via mixing palm and cottonseed oil.

Present study includes ultrasound-assisted transesterification from mixed cotton seed and palm oil feedstock, analysis of different components, and thermal stability evaluation of biodiesel resulting from mixed oil feedstock. Cotton seed and palm oils were blended in different proportions for transesterification reaction to obtain better characteristics. Finally, mixed oil composition with the best physicochemical properties and fatty acid components is selected for process parameter optimization via RSM. Furthermore, validation of optimized process parameters was performed via ANN.

2. Research Highlights

1. P60C40 biodiesel blend shows maximum calorific value as compare to other two blends.
2. The RSM and ANN results are comparable with high accuracy.
3. The maximum predicted biodiesel yield was 96.41% and the experimentally obtained yield was 96.32%.
4. The maximum training epochs and MSE were 200 and 0.0001.

3. Materials and Methods

3.1. Materials and Chemicals

Crude palm olein was obtained from Sime Darby Plantation Berhad, Malaysia. Cotton seed oil was imported from local market of Lahore, Pakistan. Methanol with 99.9% purity level and AR grade potassium hydroxide catalyst were sourced from Friendemann Schmidt and Whatman filter papers were sourced from Filtres Fioroni.

3.2. Experimental Methodology

Palm–Cotton Seed Oil Mixtures and Selection of Best Blend

The crude palm oil (PO) and cotton seed oil (CO) were blended in varying proportions to be used as a feedstock for transesterification reaction. Three different POCO mixtures were prepared with different individual oil percentages: (1) 50% PO + 50% CO, (2) 60% PO + 40% CO, 3) 70% PO + 30% CO and labeled as P50C50, P60C40 and P70C30 respectively. To obtain a homogeneous mixture, the aforementioned proportions of PO and CO were

blended for 2 h utilizing digital hotplate magnetic stirrer at 70 °C and a stirring rate of 700RPM.

Based on physicochemical properties, P60C40 oil blend was selected for the optimization of transesterification reaction. The P60C40BD showed the higher calorific value among all three biodiesel samples prepared from oil blends. The higher calorific value of P60C40BD showed that the engine will generate more power, which means low fuel consumption.

3.3. Experimental Setup for Transesterification Process

Ultrasound-assisted transesterification was executed via utilizing QSONICA (Q500 Sonicator) ultrasonic equipment. Equipment operates on 500 W maximum rated power along 20 kHz frequency and a tapered micro tip of 12.7 mm diameter probe. To obtain the optimum process parameters set, mixed palm oil and cotton seed oil biodiesel (POCOBD) was prepared by ultrasound-assisted transesterification using a 500 mL batch reactor. The calculated amount of P60C40 oil blend was taken in reactor. Mixture of KOH catalyst and methanol was prepared by mixing the solution on the stirrer plate for about 5 min to obtain a homogenized methoxide solution. The methoxide is then poured in a mixed oil blend and placed inside the sonicator. The value of ultrasound unit amplitude for all batch experiments was fixed to 40%. The following process variables were changed to study their influence on P60C40 yield: M: O (methanol-to-oil) molar ratio (30–65 v/v %), KOH catalyst percentage (0.5–1.5 wt %) and reaction time (20–50 min). After transesterification, separating funnel was employed for the settling down of impurities from reaction mixture for up to 6–7 h. Biodiesel obtained from the separating funnel was then washed with hot (70–80 °C) water to remove methanol from it until the formation of a clear water layer formed in the bottom of the separating funnel. The washed biodiesel was then heated in rotary evaporator for about 30–40 min at 70 °C and 150 rpm so that maximum impurities could be removed. Finally, the biodiesel yield was calculated via Equation (1) after filtering it through Whatman filter paper [16]. Density (at 15 °C) while kinematic viscosity (at 40 °C) was measured via a viscometer. Composition of long chain carbon element has been determined by GCMS analysis.

$$\text{Biodiesel yield \%} = \frac{\text{weight of P60C40 biodiesel}}{\text{weight of P60C40 oil blend}} \times 100 \quad (1)$$

3.4. Optimization of Biodiesel Yield

Box–Behnken with three variables was utilized to evaluate and study the response matrix along with optimum parameter combination. Yield percentage of palm cotton biodiesel is mainly depending on independent variable process parameters. Variation of all three parameters significantly affects the yield percentage of biodiesel. Optimization of parameters can help to reduce time and energy consumption which lead to maximum biodiesel yield with lowest wastage of time and also energy. Therefore, the RSM approach had been carried out to maximize the yield of palm cotton biodiesel. A total of 17 experiments were conducted for yield optimization. Ranges of operating parameters of transesterification process are demonstrated in Table 1. Equation (2) is used for biodiesel yield production via varying operating parameters.

$$Y = X_0 + \sum_{i=1}^k X_i A_i + \sum_{i=1}^k X_{ii} B_i^2 + \sum_{j=i+1}^k \cdot \sum_{i=1}^k X_{ij} C_{ij} \quad (2)$$

where,

Y = Predicted yield

A_i , B_i , and C_{ij} = Input independent variables

X_0 and X_i = Intercept and 1st order regression coefficient

X_{ii} = Quadratic regression coefficient

X_{ij} = Regression coefficient among i th and j th input parameters
 K = Independent input variables total amount

Table 1. Input process parameters for P60C40 yield optimization.

Operating Paramete	Units	Coded Factors	Coded Factors		
			−1 level	Average	+1 level
Reaction time	Minute	A	20	35	50
Methanol-to-oil ratio	Vol%/vol%	B	30	47.5	65
Concentration of catalyst	Wt%	C	0.5	1	1.5

3.5. ANN Technique

The artificial neural network (ANN) was utilized to validate RSM yield results. Actually, ANN works similar to brain neurons. Their core purpose is to analyze the yields obtained from RSM and to predict the optimum yield. ANN neurons are usually connected with their synaptic weights. Neurons are actually capable of storing the information, after which point they are trained according to assigned function (such as tansig or purelin) and hence optimum response is obtained [42].

Natural human brain neuron and structural model of ANN are mentioned in Figure 1.

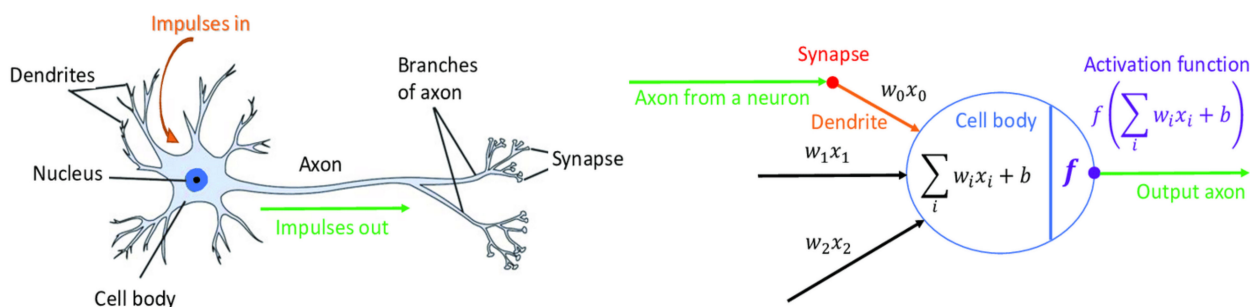


Figure 1. Natural human brain neuron and structural ANN model [43].

A combined dataset consisting of 17 data points was compiled and operating parameters of transesterification process act as independent input variables. Feed-forward backprop ANN network was selected along TRAINLM as a training function, LEARNGDM adaption learning function, and MSE as a performance function. ANN model entails three input, two hidden, and one output layers with three, three, seven, and one neurons accordingly. These layers entail transfer functions—such as logsig, tansig, and purelin—accordingly. This developed model gives a dependent variable known as biodiesel yield as a result of 17 runs of independent variables. ANN was performed on MATLAB software, 2019 version. Accuracy of models was checked by three different Equations (3)–(5).

$$MAD = \sum_{i=1}^n \frac{(|x_i - x^i|)}{n} \tag{3}$$

$$MAPE = \sum_{i=1}^n \frac{\left\{ \frac{(|x_i - x^i|)}{x_i} \right\}}{n} \tag{4}$$

$$MSE = \sum_{i=1}^n \frac{(|x_i - x^i|)}{2n} \tag{5}$$

4. Result and Discussions

4.1. Characterization of Biodiesel Blends

Physicochemical properties of PO, CO, and their blends were measured and presented in Table 1. These oil blends were then used for producing biodiesel using the ultrasound technique. The operating parameters for ultrasonic transesterification were set as follows: catalyst 1 wt %, methanol 60 wt %, time 30 min, amplitude 40%, and a 5 s on/2 s off duty cycle. Physicochemical properties of resulted POCO biodiesel samples were analyzed and listed in Table 2 to select the best oil blend for optimization. The fatty acid composition of palm and cotton seed biodiesel has been illustrated in Table 3.

Table 2. Physicochemical properties of palm and cotton oil and their methyl ester blends.

Properties	P50C50	P60C40	P70C30	P50C50BD	P60C40BD	P70C30BD
Density at 15 °C (kg/m ³)	0.9186	0.9178	0.9170	0.8792	0.8786	0.8785
Viscosity at 40 °C (mm ² /s)	36.237	38.038	38.369	4.2041	4.3058	4.5049
Acid value (mg KOH/g)	2.78	3.02	3.72	-	-	-
Calorific Value (MJ/kg)	38.81	38.86	38.27	39.12	39.23	39.01
Oxidation stability (h)	-	-	-	2.03	-	-

Table 3. Fatty acid composition of palm and cotton biodiesel.

Fatty Acid Name	Structure	PB
CB	PB + CB	
Myristic acid 0.74	0.49	0.90
Palmitic acid 25.17	32.05	38.98
Palmitoleic acid 0.57	0.37	
Stearic acid 3.02	3.63	4.04
Oleic acid 19.52	34.56	44.96
Linoleic acid 49.92	28.92	10.52
Linolenic acid -	0.26	0.39
Erucic acid 1.06	0.54	
Total saturated fatty acids 28.93	30.05	43.92
Total unsaturated fatty acids 71.07	69.95	56.08

4.2. Biodiesel Yield Optimization

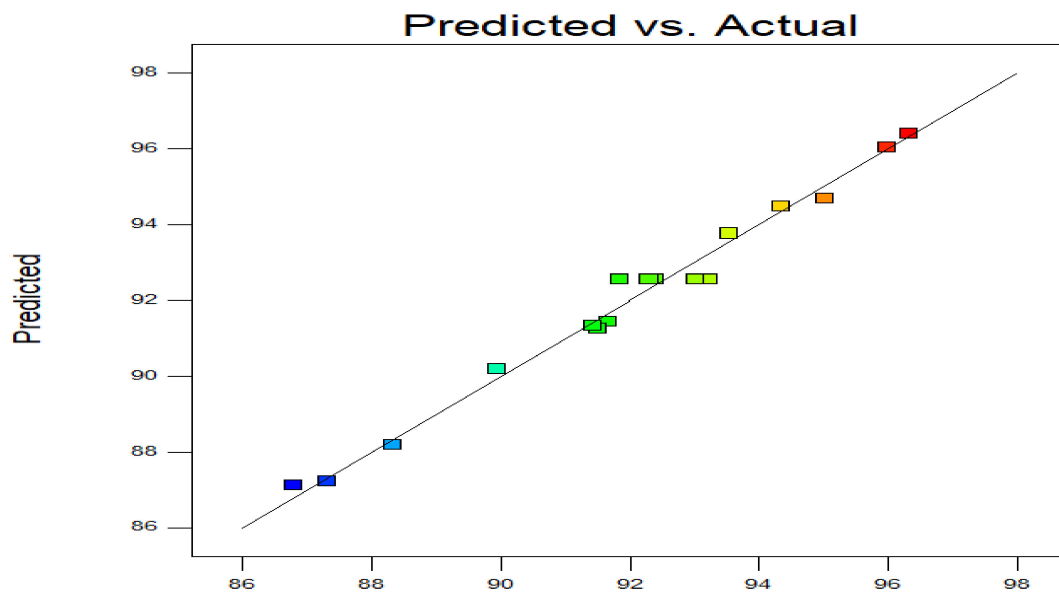
RSM develops an interaction among operating parameters of transesterification process, as the biodiesel yield mainly depends upon these operating parameters, so at optimum operating parameters the biodiesel yield would be optimum [44]. Take three input reaction variables such as time (A), methanol-to-oil ratio (B), and catalyst concentration (C). Yield of palm–cotton biodiesel was obtained for 17 experiments. Dependence of independent variables, dependent response and projected biodiesel yield has been demonstrated in Table 4. Equation (6) obtained via design expert.

$$\text{Yield} = 92.97 - 0.94 \times A - 0.3 \times B - 3.47 \times C + 0.85 \times AB - 1.12 \times AC + 0.17 \times A^2 - 0.47 \times B^2 - 0.37 \times C^2 \quad (6)$$

where A is reaction time, B is methanol-to-oil ratio, and C is catalyst concentration. Predicted versus actual yield relationship is demonstrated in Figure 2.

Table 4. Experimental design for optimization of P60C40 biodiesel yield.

Run	Time	M: O	Catalyst Concentration	Experimental Yield	Predicted Yield
	minute	(v/v %)	w/w	(%)	(%)
1	20	47.5	1.5	91.43	91.34
2	20	47.5	0.5	95.97	96.05
3	35	30	1.5	88.34	88.19
4	50	47.5	1.5	87.32	87.24
5	35	65	1.5	86.8	87.13
6	35	47.5	1	93.21	92.55
7	35	47.5	1	91.84	92.55
8	35	47.5	1	92.3	93.77
9	20	30	1	93.53	90.19
10	50	30	1	89.95	92.55
11	35	47.5	1	93.01	96.41
12	50	47.5	0.5	96.32	91.27
13	50	65	1	91.51	91.27
14	20	65	1	91.67	91.43
15	35	30	0.5	95.02	94.70
16	35	65	0.5	94.34	94.50
17	35	47.5	1	92.39	92.55

**Figure 2.** Actual vs. predicted yield for P60C40 biodiesel.

4.3. Validation of RSM Technique

ANOVA is a statistical tool which can be utilized for the yield validation as exhibited in Table 5. Model F-value of 52.87 exhibits model significance. The probability of this much larger F-value is 0.01% and it may be because of noise. Less than 0.0500 “Prob > F” values exhibit that the terms of model are significant. A, C, AB, AC, and B² in the present scenario are significant terms. The terms having values greater than 0.1000 are insignificant. A more insignificant term means that there is a model reduction requirement. “Lack of Fit F-value” of 0.56 demonstrates that it is not significant with respect to pure error. There is 67.03% probability of this large “Lack of Fit F-value” may be because of noise. Non-significant lack of fit is good.

Table 5. ANOVA results from design expert software.

Source	Sum of Squares	df	Mean Square	F Value	p-Value	
Model	119.52	9	13.28	52.87	<0.0001	significant
A-Time	7.03	1	7.03	28.00	0.0011	
B-Meth/Oil	0.79	1	0.79	3.16	0.1187	
C-Catalyst	96.33	1	96.33	383.54	<0.0001	
AB	2.92	1	2.92	11.64	0.0113	
AC	4.97	1	4.97	19.80	0.0030	
BC	0.18	1	0.18	0.74	0.4193	
A ²	0.59	1	0.59	2.36	0.1686	
B ²	6.68	1	6.68	26.62	0.0013	
C ²	0.11	1	0.11	0.46	0.5210	
Residual	1.76	7	0.25			
Lack of Fit	0.52	3	0.17	0.56	0.6703	not significant
Pure Error	1.24	4	0.31			
Cor Total	121.27	16				

4.4. Effect of Operating Parameters

Reaction parameters' effect on yield percentages is exhibited in Figure 3 in the form of 3D surface plots by keeping two of them constant at a time. Methanol-to-oil molar ratio is varied between 30 and 65 *v/v* to examine its variation impact on biodiesel yield. Figure 3 exhibits methanol-to-oil molar proportion impact on yield along with response time and catalyst concentration. It was observed that the increment of methanol-to-oil molar proportion increases yield. Furthermore, reaction temperature and catalyst concentration should also be optimized to increase solubility and improve the reaction rate [45]. At lower methanol-to-oil ratios, the reaction time increases but it decreases at higher levels of methanol yield due to excess methanol from the separation of alkyl ester and glycerol increasing solubility [46,47]. This contributes to dilution in one part of the remaining glycerol in alkyl ester process which causes ester loss due to soap formation. Likewise, glycerol presence shifts balance back to left leading to yield reduction. That is why an optimum methanol-to-oil ratio is necessary. Methanol-to-oil molar ratio of 47.5 *v/v* % gives highest yield. Elliptical form of the surface response map suggests a fairly large relationship between the surface response charts factor. Influence of concentration of catalyst (KOH) on the yield of biodiesel was determined from 0.5 to 1.5 *w/w*. Excess catalyst concentration (more than 0.5 *w/w*) can also reduce yield and cause difficulty in aqueous layer separation (more saponification) during washing. Excessive catalyst will also result in obtaining a very viscous biodiesel which cannot be used as fuel for engines. The maximum yield of biodiesel produced is obtained at 0.5 *w/w* catalyst concentration. In addition, an inadequate catalyst concentration in reaction culminated in a decrease in the production of methyl ester [48].

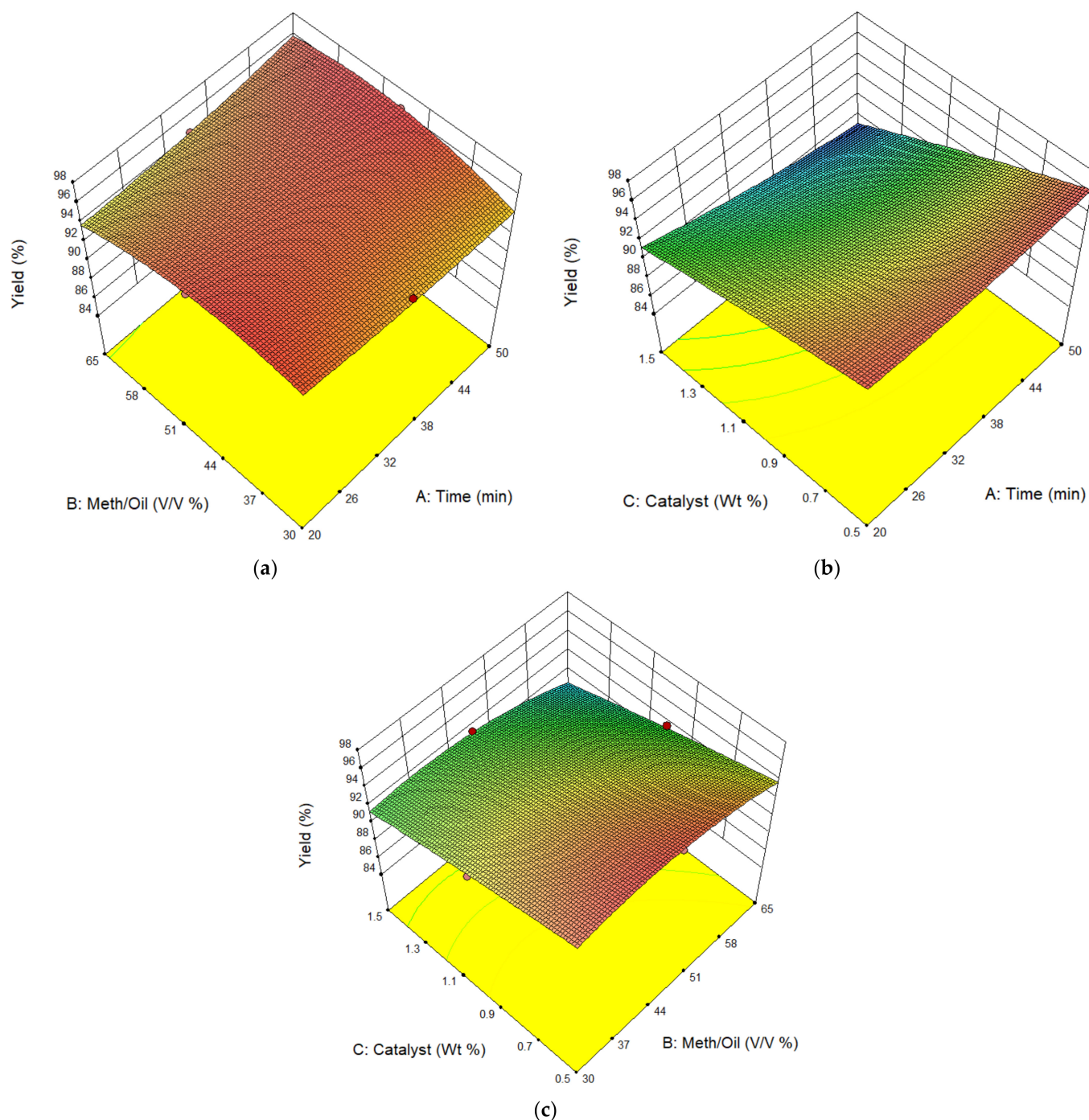


Figure 3. RSM plots for the effect of operating process variables (a) Time and Methanol to oil ratio (b) Time and catalyst (c) Methanol to oil and catalyst, on P60C40 biodiesel yield.

4.5. Validation of Results by ANN

4.5.1. Development of ANN Model

After RSM, verification and validation of output responses is conducted via artificial neural network. For this purpose, the feed-forward backprop ANN network was selected with 'TRAINLM' training function, 'LEARNGDM' Adaption learning function, and 'MSE' as a performance function. The ANN model utilized three input, two hidden, and one output layers with three, three, seven, and one neurons accordingly. These layers have transfer functions as 'logsig', 'tansig', and 'purelin', as demonstrated in Figures 4 and 5.

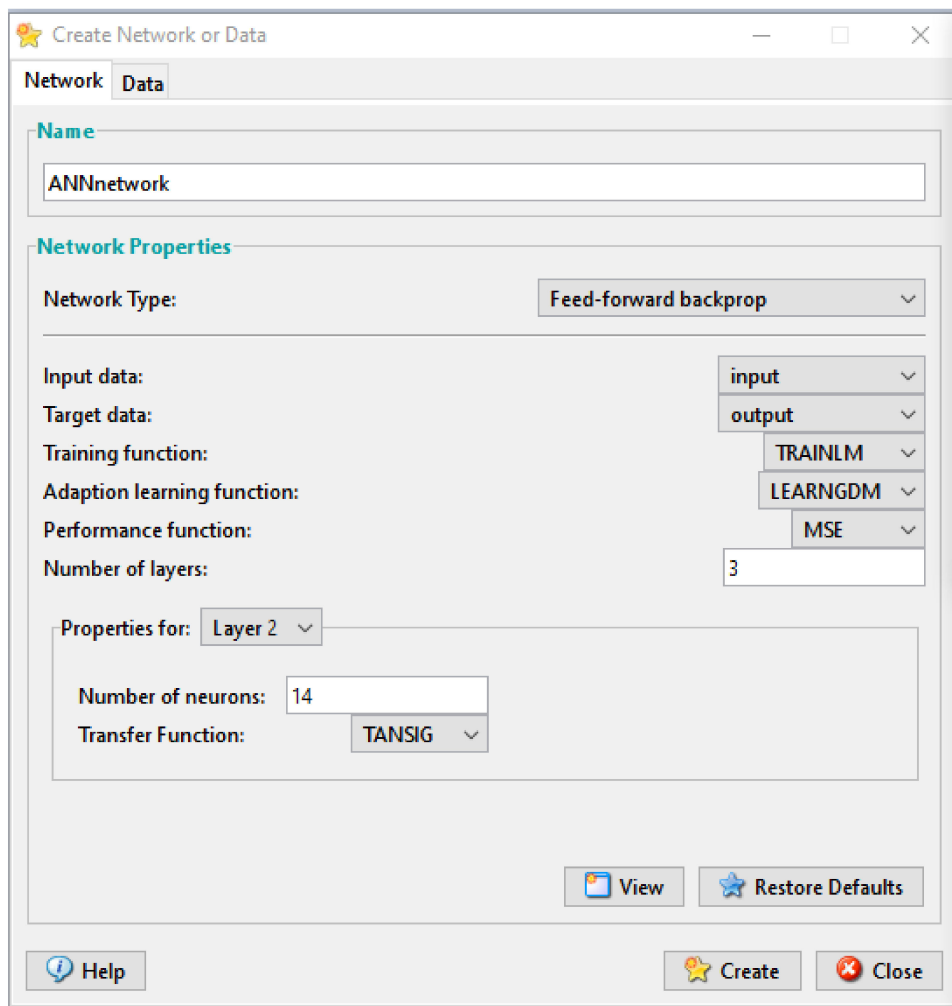


Figure 4. Development of ANN model.

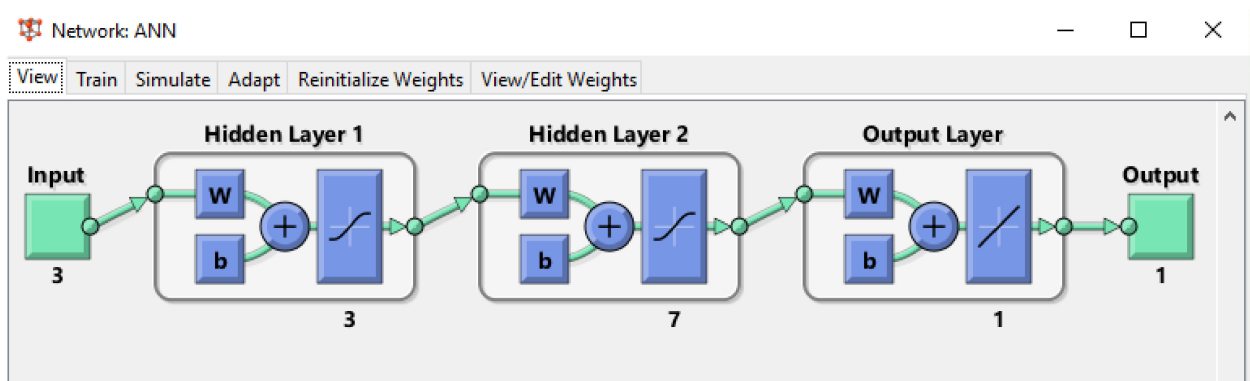


Figure 5. ANN model.

4.5.2. ANN Training

Feedforward ANN model was utilized for training via experimental data of Table 4. For network training, “trainlm” function is utilized to updates weight values and bias according to Levenberg–Marquardt optimization. Maximum training epochs are 200 and MSE is 0.0001. Other training parameters of artificial neural network are exhibited in Figure 6.

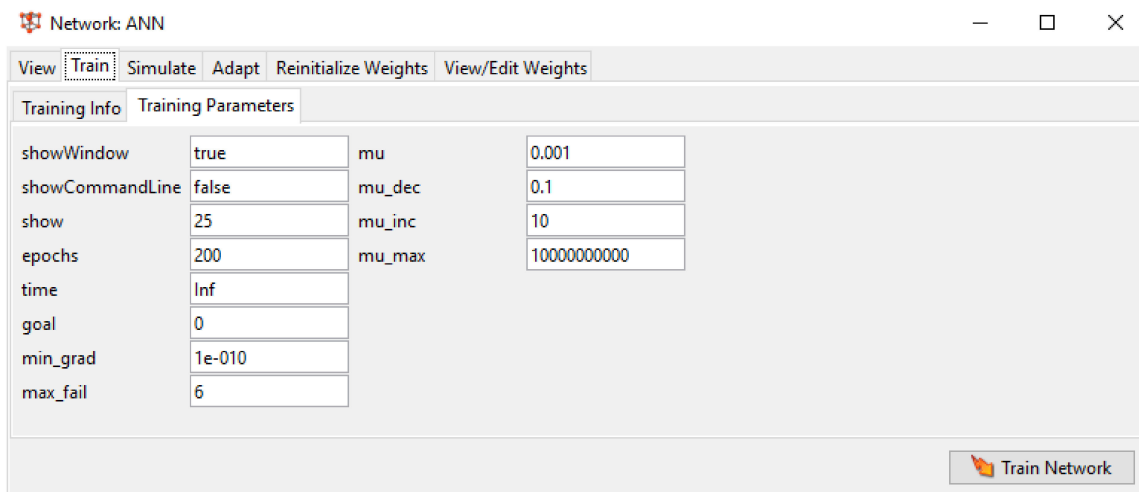


Figure 6. Training parameters.

During training, central hidden layer neurons were varied until mean square error was reduced to 1.6435×10^{-19} . Then this trained ANN was utilized to measure output (Yield %) on optimum parameter combinations as suggested by RSM (A1B3C2). Screenshots of ANN training and performance have been presented in Figures 7 and 8.

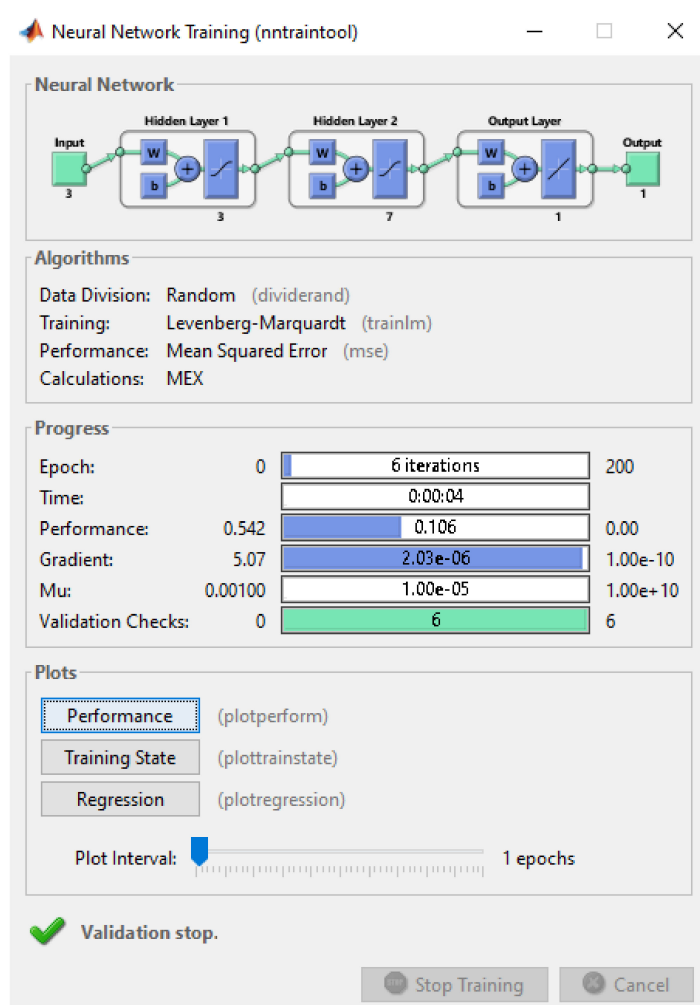


Figure 7. Training of ANN model.

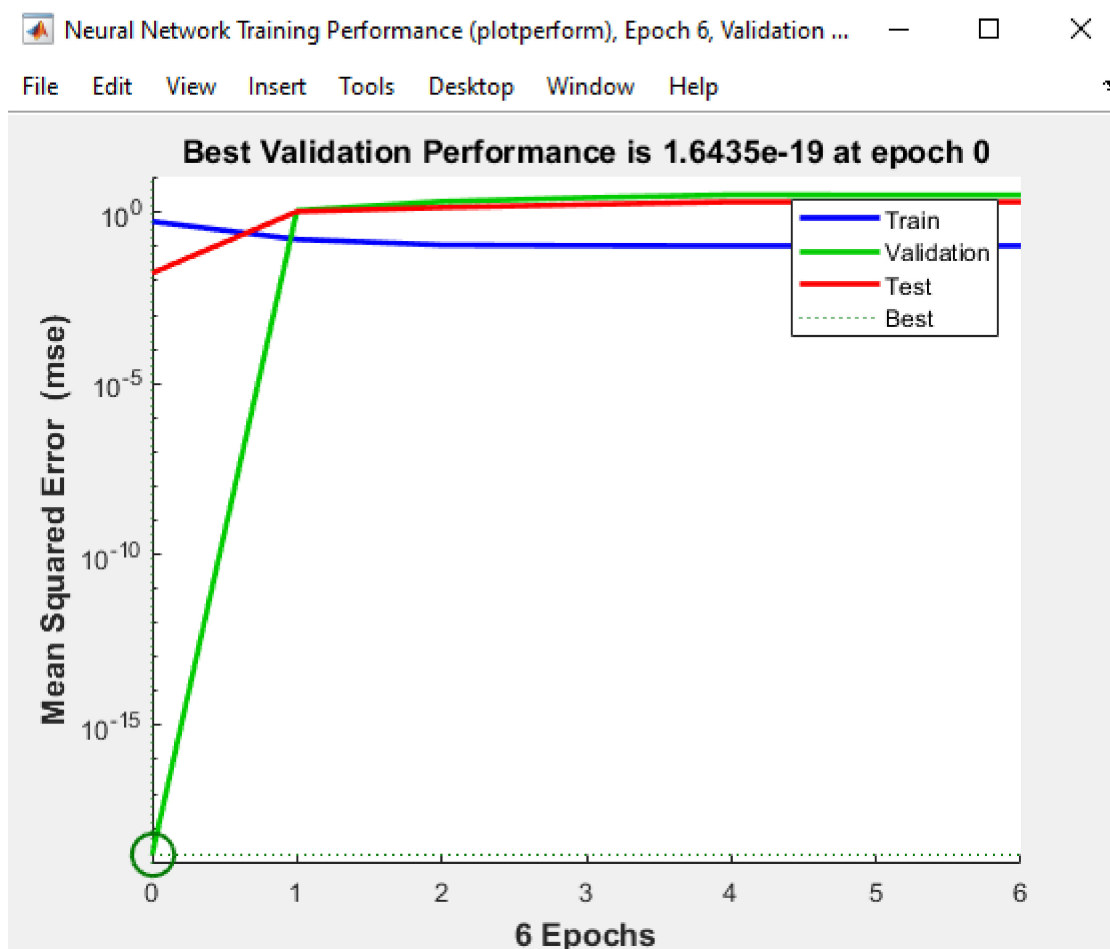


Figure 8. Performance of ANN model.

4.5.3. ANN Simulation

Finally, the trained network predicts output responses (% Biodiesel yield). Figure 9 clearly demonstrates that yield by both methods (i.e., ANN and experimental results) were almost the same, ensuring RSM effectiveness. Figure 10 represents the neural network and Figure 11 exhibits biodiesel yield obtained by ANN model which is very near to that yield obtained by experimentally and RSM model. The comparison of maximum experimentally obtained biodiesel yield was made with yield obtained by RSM and ANN model, and has been shown in Figure 12.

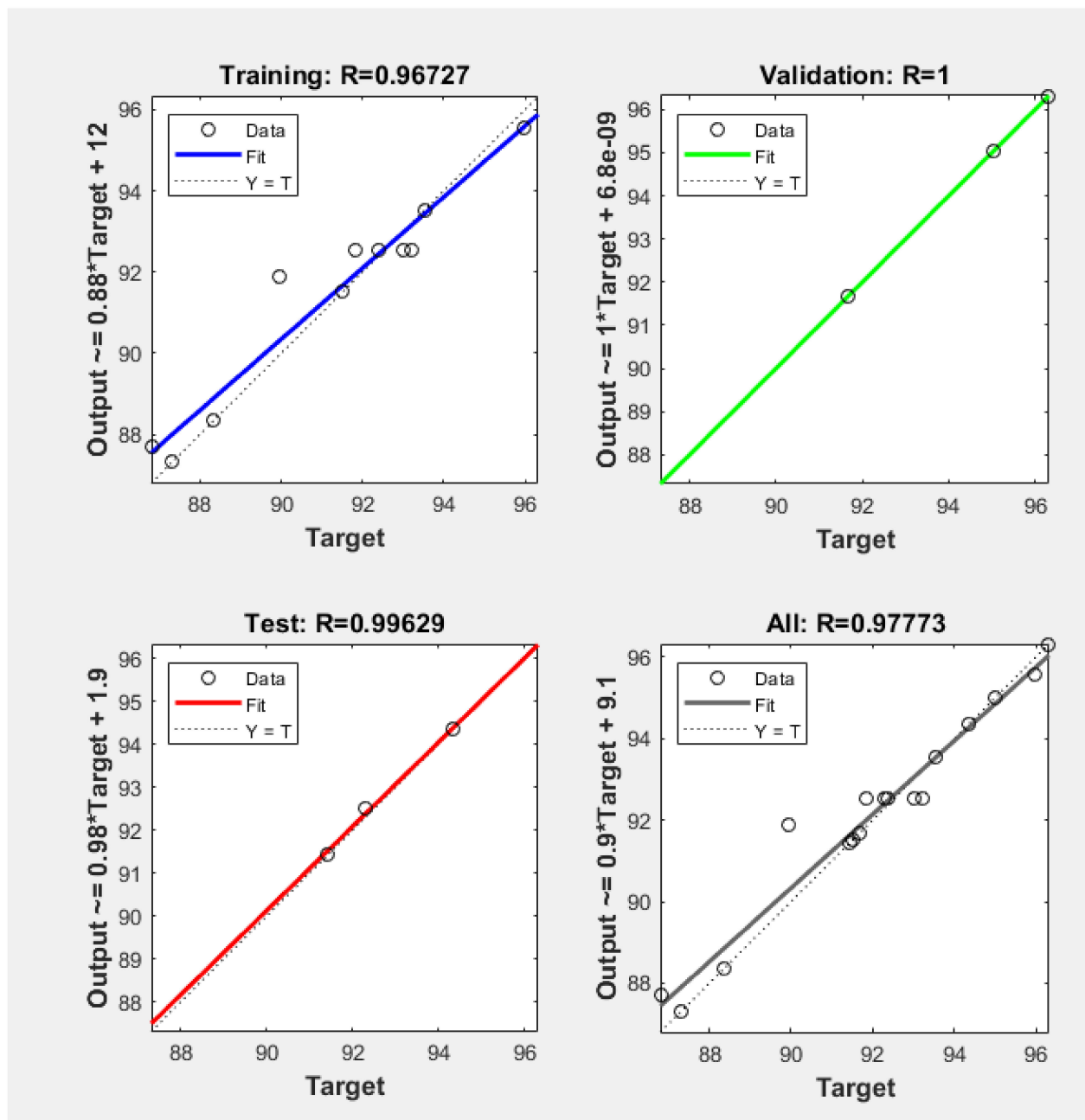


Figure 9. Regression analysis of ANN model.

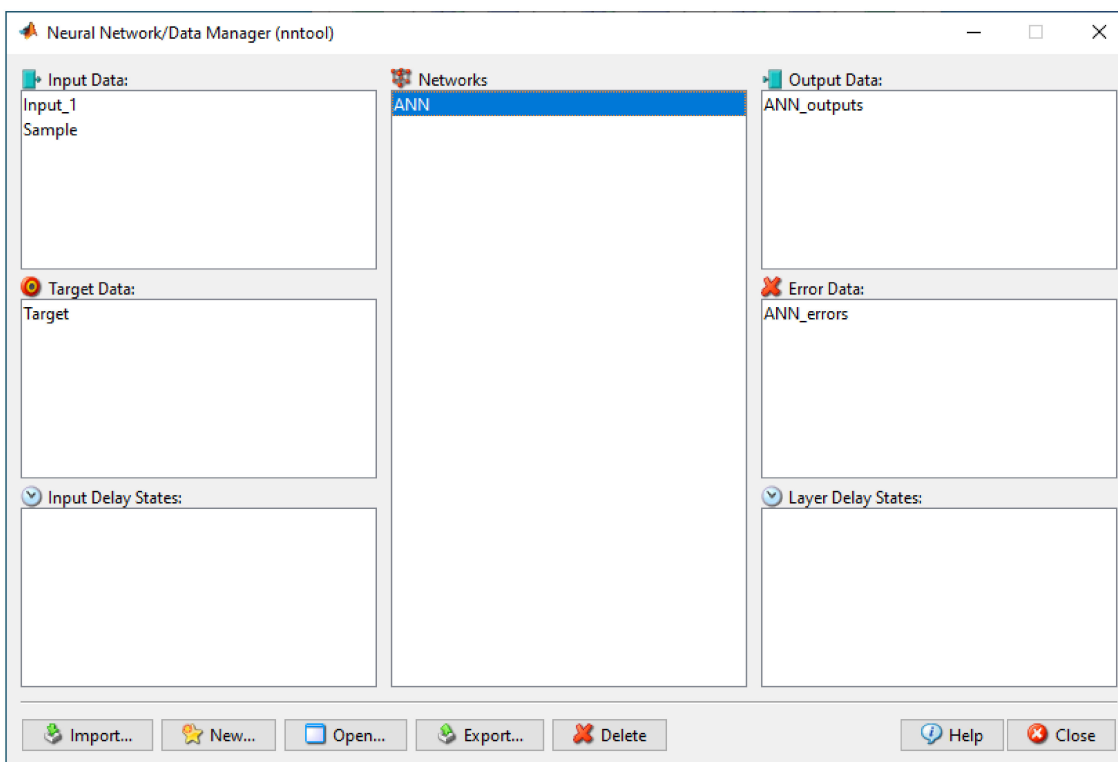


Figure 10. Neural network.

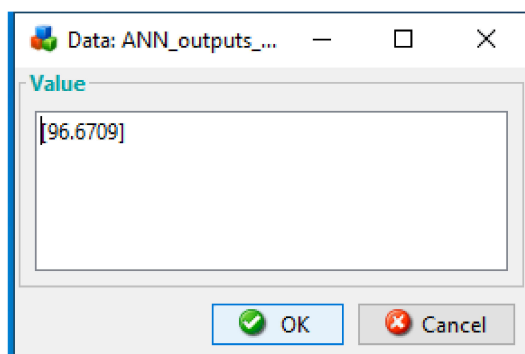


Figure 11. Output of ANN model.

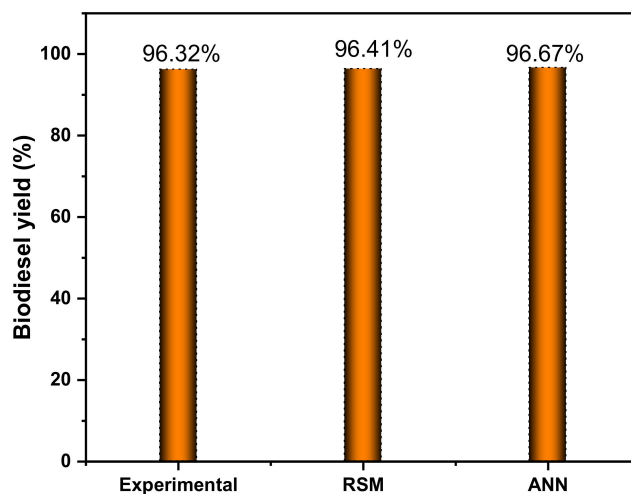


Figure 12. Comparison of experimental biodiesel yield with RSM and ANN models.

5. Conclusions

The cold flow properties of palm biodiesel and oxidation stability of cotton seed biodiesel are not good. These properties can be enhanced by mixing palm and cotton seed oil. Three different samples of palm and cotton seed oil—P50C50, P60C40 and P70C30—were prepared. The P60C40 sample has been used to investigate the yield analysis by two techniques, RSM and ANN. The maximum biodiesel yield for P60C40 was predicted as 96.41% using RSM and 96.67% using ANN under operating parameters of reaction time (35 min), methanol-to-oil molar ratio (47.5 v/v %), and catalyst concentration (1 wt %), but the actual biodiesel yield obtained experimentally was observed as being 96.32%. Physicochemical characteristics of biodiesel were analyzed regarding ASTM standards and GCMS analysis showed free fatty acid composition of P60C40 methyl ester. Both RSM and ANN have been recognized as being much faster than any predictable simulation software without extensive iteration methods of calculations in order to solve differential equations using numerical methods. Both RSM and ANN results are comparable with experimental results, a slight error of 0.09% and 0.36% has been observed in RSM and ANN models as compared to experimental results. The models developed in this research work are accurate and can be used to predict the biodiesel yield with high precision.

Author Contributions: Conceptualization, M.M.A. and M.A.K.; methodology, M.M.A.; software, L.R.; validation, M.E.M.S., N.S. and M.A.K.; formal analysis, M.M.A.; resources, M.A.K.; data curation, M.M.A.; writing—original draft preparation, L.R. and N.S.; writing—review and editing, S.M., S.A., S.K., I.V. and S.N. supervision, M.A.K.; funding acquisition, A.A. All authors have read and agreed to the published version of the manuscript.

Funding: This research received no external funding.

Conflicts of Interest: The authors declare no conflict of interest.

Nomenclature

PO	Palm oil
CO	Cotton seed oil
P50C50	50% palm oil + 50% cotton oil
P60C40	60% palm oil + 40% cotton oil
P70C30	70% palm oil + 30% cotton oil
POCOBD	Mixed palm oil and cotton seed oil biodiesel
RSM	Response surface methodology
GCMS	Gas chromatography mass spectrum
ANN	Artificial neural networks
MSE	Mean square error
MAE	Mean absolute error
MAD	Mean absolute deviation
R ²	Coefficient of determination
R	Correlation coefficient
MAPE	Mean absolute percentage error

References

- Johnston, M.; Holloway, T. Policy Analysis National Biodiesel Production Potentials. *Environ. Sci. Technol.* **2007**, *41*, 7967–7973. [[CrossRef](#)] [[PubMed](#)]
- REN21. *Renewables 2020 Global Status Report*; REN12: Paris, France, 2020.
- Razzaq, L.; Imran, S.; Anwar, Z.; Farooq, M.; Abbas, M.M.; Khan, H.M.; Asif, T.; Amjad, M.; Soudagar, M.E.M.; Shaikat, N.; et al. Maximising Yield and Engine Efficiency Using Optimised Waste Cooking Oil Biodiesel. *Energies* **2020**, *13*, 5941. [[CrossRef](#)]
- Ingeborgrud, L.; Heidenreich, S.; Ryghaug, M.; Skjølsvold, T.M.; Foulds, C.; Robison, R.; Buchmann, K.; Mourik, R. Expanding the scope and implications of energy research: A guide to key themes and concepts from the Social Sciences and Humanities. *Energy Res. Soc. Sci.* **2019**, *63*, 101398. [[CrossRef](#)]
- Mutezo, G.; Mulopo, J. A review of Africa's transition from fossil fuels to renewable energy using circular economy principles. *Renew. Sustain. Energy Rev.* **2020**, *137*, 110609. [[CrossRef](#)]

6. Hickey, W. *Energy and Human Resource Development in Developing Countries*; Springer: Berlin/Heidelberg, Germany, 2017; pp. 35–69.
7. Ong, H.C.; Masjuki, H.H.; Mahlia, T.M.I.; Silitonga, A.S.; Chong, W.T.; Yusaf, T. Engine performance and emissions using *Jatropha curcas*, *Ceiba pentandra* and *Calophyllum inophyllum* biodiesel in a CI diesel engine. *Energy* **2014**, *69*, 427–445. [CrossRef]
8. Wakil, M.; Kalam, M.; Masjuki, H.; Atabani, A.; Fattah, I.R. Influence of biodiesel blending on physicochemical properties and importance of mathematical model for predicting the properties of biodiesel blend. *Energy Convers. Manag.* **2015**, *94*, 51–67. [CrossRef]
9. Alajmi, F.S.; Hairuddin, A.A.; Adam, N.M.; Abdullah, L.C. Recent trends in biodiesel production from commonly used animal fats. *Int. J. Energy Res.* **2017**, *42*, 885–902. [CrossRef]
10. Global Biodiesel Market Report 2017–2021. Available online: <https://www.marketsandmarkets.com/Market-Reports/Global-Biodiesel-Market-190.html> (accessed on 7 January 2022).
11. Razzaq, L.; Farooq, M.; Mujtaba, M.; Sher, F.; Farhan, M.; Hassan, M.; Soudagar, M.; Atabani, A.; Kalam, M.; Imran, M. Modeling Viscosity and Density of Ethanol-Diesel-Biodiesel Ternary Blends for Sustainable Environment. *Sustainability* **2020**, *12*, 5186. [CrossRef]
12. Etim, A.O.; Musonge, P.; Eloka-Eboka, A.C. Effectiveness of biogenic waste-derived heterogeneous catalysts and feedstock hybridization techniques in biodiesel production. *Biofuels Bioprod. Biorefining* **2020**, *14*, 620–649. [CrossRef]
13. Quayson, E.; Amoah, J.; Hama, S.; Kondo, A.; Ogino, C. Immobilized lipases for biodiesel production: Current and future greening opportunities. *Renew. Sustain. Energy Rev.* **2020**, *134*, 110355. [CrossRef]
14. Bockey, D. The significance and perspective of biodiesel production—A European and global view. *OCL* **2019**, *26*, 40. [CrossRef]
15. Kim, D.-S.; Hanifzadeh, M.; Kumar, A. Trend of biodiesel feedstock and its impact on biodiesel emission characteristics. *Environ. Prog. Sustain. Energy* **2017**, *37*, 7–19. [CrossRef]
16. Mujtaba, M.; Masjuki, H.; Kalam, M.; Ong, H.C.; Gul, M.; Farooq, M.; Soudagar, M.E.M.; Ahmed, W.; Harith, M.; Yusoff, M. Ultrasound-assisted process optimization and tribological characteristics of biodiesel from palm-sesame oil via response surface methodology and extreme learning machine—Cuckoo search. *Renew. Energy* **2020**, *158*, 202–214. [CrossRef]
17. Razzaq, L.; Mujtaba, M.; Soudagar, M.E.M.; Ahmed, W.; Fayaz, H.; Bashir, S.; Fattah, I.R.; Ong, H.C.; Shahapurkar, K.; Afzal, A.; et al. Engine performance and emission characteristics of palm biodiesel blends with graphene oxide nanoplatelets and dimethyl carbonate additives. *J. Environ. Manag.* **2021**, *282*, 111917. [CrossRef]
18. Sierra-Cantor, J.F.; Guerrero-Fajardo, C.A. Methods for improving the cold flow properties of biodiesel with high saturated fatty acids content: A review. *Renew. Sustain. Energy Rev.* **2017**, *72*, 774–790. [CrossRef]
19. Mujtaba, M.A.; Masjuki, H.H.; Kalam, M.A.; Noor, F.; Farooq, M.; Ong, H.C.; Gul, M.; Soudagar, M.E.M.; Bashir, S.; Fattah, I.M.R.; et al. Effect of additivized biodiesel blends on diesel engine performance, emission, tribological characteristics, and lubricant tribology. *Energies* **2020**, *13*, 3375. [CrossRef]
20. Tan, S.X.; Lim, S.; Ong, H.C.; Pang, Y.L. State of the art review on development of ultrasound-assisted catalytic transesterification process for biodiesel production. *Fuel* **2018**, *235*, 886–907. [CrossRef]
21. Yin, X.; Ma, H.; You, Q.; Wang, Z.; Chang, J. Comparison of four different enhancing methods for preparing biodiesel through transesterification of sunflower oil. *Appl. Energy* **2012**, *91*, 320–325. [CrossRef]
22. Martinez-Guerra, E.; Gude, V.G. Determining optimum pulse mode for ultrasound enhanced biodiesel production. *J. Ind. Eng. Chem.* **2016**, *35*, 14–19. [CrossRef]
23. Latchubugata, C.S.; Kondapaneni, R.V.; Patluri, K.K.; Virendra, U.; Vedantam, S. Kinetics and optimization studies using Response Surface Methodology in biodiesel production using heterogeneous catalyst. *Chem. Eng. Res. Des.* **2018**, *135*, 129–139. [CrossRef]
24. Pali, H.S.; Sharma, A.; Kumar, N.; Singh, Y. Biodiesel yield and properties optimization from Kusum oil by RSM. *Fuel* **2021**, *291*, 120218. [CrossRef]
25. Muthukumar, C.; Praniash, R.; Navamani, P.; Swathi, R.; Sharmila, G.; Manoj Kumar, N. Process optimization and kinetic modeling of biodiesel production using non-edible *Madhuca indica* oil. *Fuel* **2017**, *195*, 217–225. [CrossRef]
26. Milano, J.; Ong, H.C.; Masjuki, H.; Silitonga, A.; Chen, W.-H.; Kusumo, F.; Dharma, S.; Sebayang, A. Optimization of biodiesel production by microwave irradiation-assisted transesterification for waste cooking oil-*Calophyllum inophyllum* oil via response surface methodology. *Energy Convers. Manag.* **2018**, *158*, 400–415. [CrossRef]
27. Dwivedi, G.; Sharma, M. Application of Box–Behnken design in optimization of biodiesel yield from *Pongamia* oil and its stability analysis. *Fuel* **2015**, *145*, 256–262. [CrossRef]
28. Niju, S.; Rabia, R.; Devi, K.S.; Kumar, M.N.; Balajii, M. Modified *Malleus malleus* Shells for Biodiesel Production from Waste Cooking Oil: An Optimization Study Using Box–Behnken Design. *Waste Biomass Valorization* **2018**, *11*, 793–806. [CrossRef]
29. Chhabra, M.; Saini, B.S.; Dwivedi, G. Optimization of the dual stage procedure of biodiesel synthesis from *Neem* oil using RSM based Box Behnken design. *Energy Sources Part A Recover. Util. Environ. Eff.* **2020**, 1–24. [CrossRef]
30. Veljković, V.B.; Veličković, A.V.; Avramović, J.M.; Stamenković, O.S. Modeling of biodiesel production: Performance comparison of Box–Behnken, face central composite and full factorial design. *Chin. J. Chem. Eng.* **2018**, *27*, 1690–1698. [CrossRef]
31. Srikanth, H.V.; Venkatesh, J.; Godiganur, S. Box-Behnken Response Surface Methodology for Optimization of Process Parameters for Dairy Washed Milk Scum Biodiesel Production. *Biofuels* **2018**, *12*, 113–123. [CrossRef]
32. Tran-Nguyen, P.L.; Ong, L.K.; Go, A.W.; Ju, Y.; Angkawijaya, A.E. Non-catalytic and heterogeneous acid/base-catalyzed biodiesel production: Recent and future developments. *Asia Pac. J. Chem. Eng.* **2020**, *15*, e2490. [CrossRef]

33. Laskar, I.B.; Deshmukhya, T.; Biswas, A.; Paul, B.; Changmai, B.; Gupta, R.; Chatterjee, S.; Rokhum, S.L. Utilization of biowaste-derived catalysts for biodiesel production: Process optimization using response surface methodology and particle swarm optimization method. *Energy Adv.* **2022**. [[CrossRef](#)]
34. Venkatesan, H.; Nalarajan, B.; Sivamani, S.; Thomai, M.P. Optimizing the process parameters to maximize palm stearin wax biodiesel yield using response surface methodology. *Energy Sources Part A Recover. Util. Environ. Eff.* **2020**, 1–19. [[CrossRef](#)]
35. Betiku, E.; Ajala, S.O. Modeling and optimization of Thevetia peruviana (yellow oleander) oil biodiesel synthesis via Musa paradisical (plantain) peels as heterogeneous base catalyst: A case of artificial neural network vs. response surface methodology. *Ind. Crop. Prod.* **2014**, *53*, 314–322. [[CrossRef](#)]
36. Betiku, E.; Omilakin, O.R.; Ajala, S.O.; Okeleye, A.A.; Taiwo, A.E.; Solomon, B.O. Mathematical modeling and process parameters optimization studies by artificial neural network and response surface methodology: A case of non-edible neem (*Azadirachta indica*) seed oil biodiesel synthesis. *Energy* **2014**, *72*, 266–273. [[CrossRef](#)]
37. Shen, C.; Wang, L.; Li, Q. Optimization of injection molding process parameters using combination of artificial neural network and genetic algorithm method. *J. Mater. Process. Technol.* **2007**, *183*, 412–418. [[CrossRef](#)]
38. Rajendra, M.; Jena, P.C.; Raheman, H. Prediction of optimized pretreatment process parameters for biodiesel production using ANN and GA. *Fuel* **2009**, *88*, 868–875. [[CrossRef](#)]
39. Ong, H.C.; Milano, J.; Silitonga, A.S.; Hassan, M.H.; Shamsuddin, A.H.; Wang, C.-T.; Mahlia, T.M.I.; Siswanto, J.; Kusumo, F.; Sutrisno, J. Biodiesel production from Calophyllum inophyllum-Ceiba pentandra oil mixture: Optimization and characterization. *J. Clean. Prod.* **2019**, *219*, 183–198. [[CrossRef](#)]
40. Shuli, F.; Jarwar, A.H.; Wang, X.; Wang, L.; Ma, Q. Overview of the Cotton in Pakistan and its Future Prospects. *Pak. J. Agric. Res.* **2018**, *31*, 291–418. [[CrossRef](#)]
41. Yesilyurt, M.K.; Aydin, M. Experimental investigation on the performance, combustion and exhaust emission characteristics of a compression-ignition engine fueled with cottonseed oil biodiesel/diethyl ether/diesel fuel blends. *Energy Convers. Manag.* **2019**, *205*, 112355. [[CrossRef](#)]
42. Gul, M.; Shah, A.N.; Aziz, U.; Husnain, N.; Mujtaba, M.A.; Kousar, T.; Ahmad, R.; Hanif, M.F. Grey-Taguchi and ANN based optimization of a better performing low-emission diesel engine fueled with biodiesel. *Energy Sources Part A Recover. Util. Environ. Eff.* **2019**, *44*, 1019–1032. [[CrossRef](#)]
43. Chang, C.-M.; Lin, T.-K.; Chang, C.-W. Applications of neural network models for structural health monitoring based on derived modal properties. *Measurement* **2018**, *129*, 457–470. [[CrossRef](#)]
44. Fayaz, H.; Mujtaba, M.; Soudagar, M.E.M.; Razzaq, L.; Nawaz, S.; Nawaz, M.A.; Farooq, M.; Afzal, A.; Ahmed, W.; Khan, T.Y.; et al. Collective effect of ternary nano fuel blends on the diesel engine performance and emissions characteristics. *Fuel* **2021**, *293*, 120420. [[CrossRef](#)]
45. Sahoo, P.; Das, L. Combustion analysis of Jatropha, Karanja and Polanga based biodiesel as fuel in a diesel engine. *Fuel* **2009**, *88*, 994–999. [[CrossRef](#)]
46. Ala'a, H.; Jamil, F.; Al-Haj, L.; Myint, M.T.Z.; Mahmoud, E.; Ahmad, M.N.; Hasan, A.O.; Rafiq, S. Biodiesel production over a catalyst prepared from biomass-derived waste date pits. *Biotechnol. Rep.* **2018**, *20*, e00284.
47. Okoye, U.; Longoria, A.; Sebastian, P.; Wang, S.; Li, S.; Hameed, B. A review on recent trends in reactor systems and azeotrope separation strategies for catalytic conversion of biodiesel-derived glycerol. *Sci. Total Environ.* **2019**, *719*, 134595. [[CrossRef](#)] [[PubMed](#)]
48. Knothe, G. Dependence of biodiesel fuel properties on the structure of fatty acid alkyl esters. *Fuel Process. Technol.* **2005**, *86*, 1059–1070. [[CrossRef](#)]